annalise

Annalise Enterprise

# Performance Guide

English

# Annalise Enterprise Product

This guide is applicable to Annalise Enterprise Backend version: 3.0 and 3.1

Date of issue: 2022-08-30



ANNALISE-AI PTY LTD
ACN 635 645 260
Level 21, 60 Margaret Street,
Sydney NSW 2000
AUSTRALIA
www.annalise.ai

QualRep Services B.V.
Utrechtseweg 310 - Bldg B42
NL-6812 AR Arnhem
THE NETHERLANDS

New Zealand Sponsor
AA-Med NZ Ltd.
Level 7, 54 Gill Street
New Plymouth, 4310
NEW ZEALAND

Malaysia Authorised Representative
ARQon Medtech Sdn Bhd
No. 20, Jalan Sasa 4
Taman Gaya, 81800, Johor
MALAYSIA
Registration Number: GA5216421-60402

UK Responsible Person
Qserve Group UK, Ltd.
49 Greek Street
Soho, London W1D 4EG
UNITED KINGDOM

Indian Voluntary Registration Number
Annali-AUS/I/MD/003060

# Product use

| | |
|---|---|
| Intended purpose | Annalise Enterprise is a medical device intended to assist clinicians with the interpretation of radiological imaging studies and provide notification of suspected findings. |
| Indications for use | Annalise Enterprise identifies suspected findings in:<br>• digitised (CR) or digital (DX) chest X-ray studies taken in the anterior-posterior (AP) or posterior-anterior (PA) and optionally lateral (LAT) orientations of adult patients<br>• non-contrast brain CT scans (brain kernel) of adult patients<br>For chest X-ray (CXR), the device improves the detection of radiological findings visible on chest X-rays. For CT Brain (CTB), the device improves the detection of radiological findings visible on non-contrast CT brain scans.<br>The device identifies 124 CXR findings and 130 CTB findings.<br>The device is used on a PC workstation in conjunction with a medical imaging viewer (i.e. PACS system).<br>The device may also be configured to provide input to worklist software to assist with notification and triaging. The device identifies studies with selected findings and communicates these studies to the worklist software which enables triaging of the worklist and notification.<br>Note: Worklist Triage and CTB are additional licenced options and are not available in all regions. |
| Intended user | The device is intended to be used by trained clinicians who are qualified to interpret chest X-rays and/or CT scans as part of their scope of practice. |
| Intended patient population | The intended population is:<br>• CXR: Patients who are 16 years or older<br>• CTB: Patients who are 18 years or older |
| Contraindications | The device:<br>• is not intended to provide direct diagnosis<br>• is not to be used on patients under the age of 16 years for CXR and under the age of 18 years for CTB<br>• does not enable an increase in the clinician's scope of practice |

## WARNING

Qualified clinicians who interpret chest X-rays and or brain CT scans as part of their scope of practice hold ultimate responsibility for interpreting studies.

The clinician must review the Annalise Enterprise output concurrently with the original chest X-ray images or brain CT scan and all other relevant clinical information before making their clinical decisions.

 

# Annalise Enterprise performance

## Overview

This document outlines the product performance of Annalise Enterprise.

For general user information, refer to the *Annalise Enterprise User Guide*.

## AUC by findings (CXR)

The following tables include all supported findings for Annalise Enterprise (CXR) in alphabetical order. Each row displays both the finding name and the area under the curve (AUC) mean.

These performance results are based on the dataset used by annalise.ai to evaluate the product. Differences in transfer syntax, demographics, imaging equipment or other variables may result in changes in performance.

*CXR findings*

| Finding | AUC |
|---|---|
| abdominal clips | 0.978 |
| acute clavicle fracture | 0.960 |
| acute humerus fracture | 0.974 |
| acute rib fracture | 0.969 |
| airway stent | 0.966 |
| aortic arch calcification | 0.976 |
| aortic stent | 0.994 |
| atelectasis | 0.882 |
| axillary clips | 0.997 |
| basal interstitial thickening | 0.887 |
| biliary stent | 0.999 |
| breast implant | 0.996 |
| bronchiectasis | 0.928 |
| calcified axillary nodes | 0.978 |
| calcified granuloma (< 5mm) | 0.930 |
| calcified hilar lymphadenopathy | 0.891 |
| calcified mass (> 5mm) | 0.953 |
| calcified neck nodes | 0.932 |
| calcified pleural plaques | 0.981 |
| cardiac valve prosthesis | 0.997 |
| cavitating mass with content | 0.971 |

***continued***

*CXR findings (cont.)*

| Finding | AUC |
|---|---|
| cavitating mass(es) | 0.928 |
| cervical flexion | 0.992 |
| chronic clavicle fracture | 0.963 |
| chronic humerus fracture | 0.988 |
| chronic rib fracture | 0.948 |
| clavicle fixation | 0.997 |
| clavicle lesion | 0.966 |
| coronary stent | 0.966 |
| diaphragmatic elevation | 0.934 |
| diaphragmatic eventration | 0.983 |
| diffuse airspace opacity | 0.979 |
| diffuse bullae | 0.969 |
| diffuse fibrotic volume loss | 0.960 |
| diffuse interstitial thickening | 0.938 |
| diffuse lower airspace opacity | 0.933 |
| diffuse nodular/miliary lesions | 0.979 |
| diffuse pleural thickening | 0.963 |
| diffuse spinal osteophytes | 0.987 |
| diffuse upper airspace opacity | 0.978 |
| distended bowel | 0.979 |
| electronic cardiac devices | 1.000 |
| focal airspace opacity | 0.852 |
| gallstones | 0.871 |
| gastric band | 0.974 |
| hiatus hernia | 0.991 |
| hilar lymphadenopathy | 0.937 |
| humeral lesion | 0.976 |
| hyperinflation | 0.965 |
| image obscured | 0.937 |
| in position central line (cvc) | 0.995 |
| in position endotracheal tube (ett) | 0.997 |
| in position nasogastric tube (ngt) | 0.997 |
| in position pulmonary arterial catheter (pac) | 0.992 |
| incompletely imaged chest | 0.981 |

***continued***

*CXR findings (cont.)*

| Finding | AUC |
|---|---|
| inferior mediastinal mass | 0.969 |
| intercostal drain | 0.997 |
| internal foreign body | 0.933 |
| kyphosis | 0.976 |
| loculated effusion | 0.952 |
| lower zone bullae | 0.954 |
| lower zone fibrotic volume loss | 0.923 |
| lung collapse | 0.997 |
| lung sutures | 0.966 |
| mastectomy | 0.962 |
| mediastinal clips | 0.993 |
| multifocal airspace opacity | 0.896 |
| multiple masses or nodules | 0.957 |
| neck clips | 0.987 |
| nipple shadow | 0.971 |
| oesophageal stent | 0.998 |
| osteopaenia | 0.955 |
| overexposed | 0.917 |
| patient rotation | 0.910 |
| pectus carinatum | 0.900 |
| pectus excavatum | 0.994 |
| peribronchial cuffing | 0.836 |
| pericardial fat pad | 0.926 |
| perihilar airspace opacity | 0.943 |
| pleural mass | 0.949 |
| pneumomediastinum | 0.969 |
| post resection volume loss | 0.980 |
| pulmonary artery enlargement | 0.942 |
| pulmonary congestion | 0.926 |
| reduced lung markings | 0.955 |
| rib fixation | 0.991 |
| rib lesion | 0.971 |
| rib resection | 0.986 |
| rotator cuff anchor | 1.000 |

***continued***

*CXR findings (cont.)*

| Finding | AUC |
|---|---|
| scapular fracture | 0.942 |
| scapular lesion | 0.951 |
| scoliosis | 0.954 |
| segmental collapse | 0.911 |
| shoulder arthritis | 0.983 |
| shoulder dislocation | 0.966 |
| shoulder fixation | 0.997 |
| shoulder replacement | 1.000 |
| simple effusion | 0.951 |
| simple pneumothorax | 0.980 |
| solitary lung mass | 0.946 |
| solitary lung nodule | 0.897 |
| spinal arthritis | 0.938 |
| spinal fixation | 0.999 |
| spinal lesion | 0.971 |
| spinal wedge fracture | 0.967 |
| sternotomy wires | 1.000 |
| subcutaneous emphysema | 0.997 |
| subdiaphragmatic gas | 0.996 |
| suboptimal central line (cvc) | 0.975 |
| suboptimal gastric band | 0.997 |
| suboptimal nasogastric tube (ngt) | 0.985 |
| suboptimal endotracheal tube (ett) | 0.995 |
| suboptimal pulmonary arterial catheter (pac) | 0.993 |
| superior mediastinal mass | 0.952 |
| tension pneumothorax | 0.997 |
| tracheal deviation | 0.951 |
| underexposed | 0.946 |
| underinflation | 0.973 |
| unfolded aorta | 0.896 |
| upper interstitial thickening | 0.900 |
| upper zone bullae | 0.964 |
| upper zone fibrotic volume loss | 0.976 |
| widened aortic contour | 0.981 |
| widened cardiac silhouette | 0.951 |

AUC by findings (CTB)

The following tables include all supported findings for Annalise Enterprise (CTB) in alphabetical order. Each row displays both the finding name and the area under the curve (AUC) mean.

These performance results are based on the dataset used by annalise.ai to evaluate the product. Differences in transfer syntax, demographics, imaging equipment or other variables may result in changes in performance.

*CTB findings*

| Finding | AUC |
|---|---|
| Abnormal prominent vessels | 0.850 |
| Acute brainstem infarct | 0.830 |
| Acute cerebellar infarct | 0.925 |
| Acute cerebral infarct | 0.923 |
| Acute haemorrhagic infarct | 0.988 |
| Acute infarct petechial haemorrhage | 0.963 |
| Acute intraparenchymal haemorrhage | 0.985 |
| Acute lacunar infarct | 0.840 |
| Acute on chronic subdural haematoma | 0.993 |
| Acute peripheral infarct | 0.887 |
| Acute subdural/extradural haematoma | 0.974 |
| Acute watershed infarct | 0.920 |
| Aggressive bone lesion | 0.887 |
| Aggressive extra-axial mass of soft tissue | 0.979 |
| Aggressive meningeal thickening | 0.913 |
| Aggressive skin lesion | 0.969 |
| Air fluid level paranasal sinuses | 0.948 |
| Aneurysm | 0.811 |
| Aneurysm coils | 0.998 |
| Arachnoid cyst | 0.964 |
| Basal ganglia and dentate calcification | 0.970 |
| Cerebellar atrophy | 0.922 |
| Cerebral atrophy | 0.884 |
| Cerebral convexity subarachnoid haemorrhage | 0.966 |
| Chiari malformation | 0.985 |
| Chronic globe abnormality | 0.927 |
| Chronic or fungal sinusitis | 0.969 |
| Chronic subdural haematoma | 0.980 |

***continued***

*CTB findings (cont.)*

| Finding | AUC |
|---|---|
| Cochlear implant | 1.000 |
| Colloid cyst | 0.998 |
| Colpocephaly | 0.991 |
| Communicating hydrocephalus/NPH | 0.974 |
| Corpus callosum agenesis/hypogenesis | 0.988 |
| Cortical laminar necrosis | 0.942 |
| Cortical or leptomeningeal calcification | 0.952 |
| Craniotomy extra-axial collection | 0.988 |
| Craniotomy/cranioplasty/craniectomy | 0.994 |
| Deep brain stimulation electrodes | 1.000 |
| Deep white or grey matter infarct | 0.948 |
| Diffuse hypoxic-ischaemic encephalopathy | 0.988 |
| Dilated superior opthalmic vein | 0.885 |
| Disappearing basal ganglia sign | 0.956 |
| Dural calcification | 0.947 |
| Effacement of basal cisterns | 0.971 |
| Empty sella | 0.950 |
| Encephalomalacia | 0.961 |
| Entrapment of lateral ventricle | 0.981 |
| Erosion of bone in tympanic cavity | 0.988 |
| Exophthalmos | 0.970 |
| Expanded pituitary fossa | 0.983 |
| Extracranial herniation | 0.952 |
| Extracranial Ventricular Drain (EVD) | 0.994 |
| Extradural haematoma | 0.937 |
| Face and neck haematomas | 0.961 |
| Focal intra-axial calcification | 0.905 |
| Foreign body face and neck | 0.906 |
| Foreign body orbit | 0.907 |
| Foreign body scalp | 0.848 |
| Fourth ventricular effacement | 0.979 |
| Fracture of calvarium | 0.960 |
| Fracture of skull base | 0.949 |
| Fracture paranasal sinuses/facial bones | 0.935 |

***continued***

*CTB findings (cont.)*

| Finding | AUC |
|---|---|
| Generalised calvarial thickening | 0.976 |
| Haemorrhagic contusion | 0.980 |
| Haemorrhagic lesion in sella | 0.899 |
| Hyperdense artery in anterior circulation | 0.954 |
| Hyperostosis frontalis | 0.987 |
| Hypopneumatised mastoid | 0.978 |
| Insular ribbon sign | 0.959 |
| Intraaxial lesion calcification | 0.978 |
| Intraaxial lesion complex cyst | 0.932 |
| Intraaxial lesion haemorrhage | 0.975 |
| Intraaxial lesion heterogeneous | 0.979 |
| Intraaxial lesion hyperdense | 0.961 |
| Intraaxial lesion hypodense | 0.929 |
| Intraaxial lesion isodense | 0.917 |
| Intra-ocular silicone | 0.998 |
| Intra-ventricular haemorrhage | 0.991 |
| Left/Right ventricular effacement | 0.978 |
| Mastoid opacification | 0.907 |
| Mastoidectomy | 0.996 |
| Meningioma with hyperostosis of adjacent calvarium | 0.959 |
| Metallic artefact | 0.968 |
| Midline shift | 0.980 |
| Movement artefact | 0.910 |
| Mucosal thickening | 0.918 |
| Non-aggressive extra-axial mass containing calcification | 0.934 |
| Non-aggressive extra-axial mass without calcification or fat | 0.843 |
| Non-aggressive skin lesion | 0.866 |
| Obstructive hydrocephalus | 0.981 |
| Old lacunar infarct | 0.915 |
| Opacity in tympanic cavity | 0.987 |
| Orbital fat stranding | 0.954 |
| Orbital mass benign | 0.905 |
| Orbital mass inflammatory or malignant | 0.967 |
| Osteoma | 0.864 |

***continued***

*CTB findings (cont.)*

| Finding | AUC |
|---|---|
| Parotid lesion | 0.843 |
| Perimesencephalic/aneurysmal subarachnoid haemorrhage | 0.987 |
| Petrous bone fracture | 0.934 |
| Pineal mass or complex cyst | 0.842 |
| Pneumocephalus | 0.940 |
| Prominent perivascular spaces | 0.873 |
| Prosthetic globe | 0.996 |
| Resection cavity | 0.982 |
| Scalp haematomas | 0.963 |
| Sella or suprasellar cyst, mass or cystic mass | 0.965 |
| Simple pineal cyst | 0.937 |
| Sino-nasal, oral, mandibular and maxillofacial surgery | 0.905 |
| Sinus soft tissue density lesion | 0.930 |
| Small vessel ischaemic disease | 0.937 |
| Soft tissue mass in the neck | 0.906 |
| Striatocapsular slit-like chronic hemorrhage | 0.971 |
| Subacute intraparenchymal haemorrhage | 0.925 |
| Subacute subdural haematoma | 0.979 |
| Subcutaneous emphysema | 0.936 |
| Subependymal calcification or nodules | 0.867 |
| Sulcal effacement | 0.966 |
| Temporomandibular joint arthritis | 0.851 |
| Temporomandibular joint dislocation | 0.969 |
| Third ventricular effacement | 0.984 |
| Tonsillar herniation | 0.993 |
| Transependymal oedema | 0.981 |
| Transphenoidal surgery | 0.957 |
| Uncal herniation | 0.993 |
| Vascular clips | 0.984 |
| Vasogenic oedema | 0.977 |
| Ventricular cyst/xanthogranulomatous change | 0.871 |
| Ventricular mass | 0.821 |
| Ventriculoperitoneal (VP) Shunt | 0.998 |
| Vitreous haemorrhage | 0.974 |

# Model validation dataset characteristics

Dataset characteristics (CXR)

The Annalise Enterprise product is validated on over 2,500 studies (both lossless transfer syntax and lossy transfer syntax) acquired from clinics across Australia and the United States of America.

Demographics of the overall test dataset:

- Patients: 2286
- Studies: 2568
- Images: 4568
- Sex: 29% male, 28% female, 43% unknown*
- Mean Age: 74 years, (standard deviation 15 years)*
- View Position: 28% posterior-anterior (PA), 33% anterior-posterior (AP), 31% optionally lateral (LAT), 8% other

*As MIMIC-CXR does not provide sex or age information, data for this is incomplete.

*Dataset of origin*

Dataset of origin of images were obtained from I-MED and the publicly available MIMIC dataset.

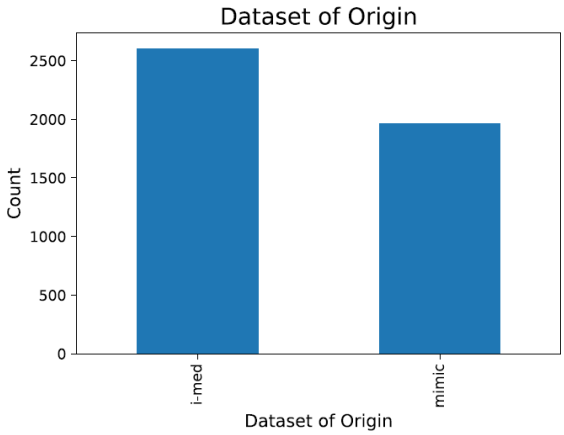


*Patient age*

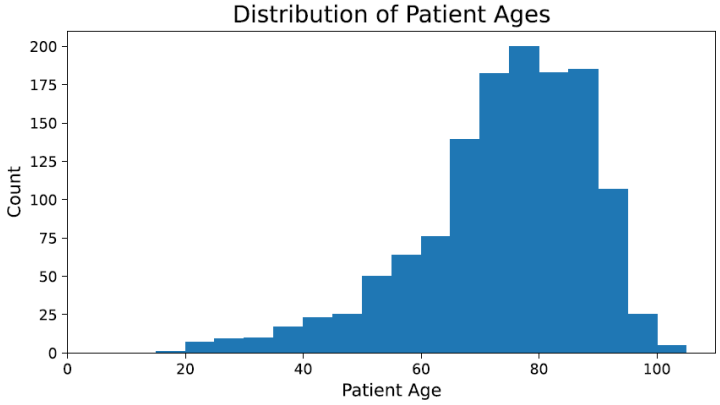

*Patient sex*

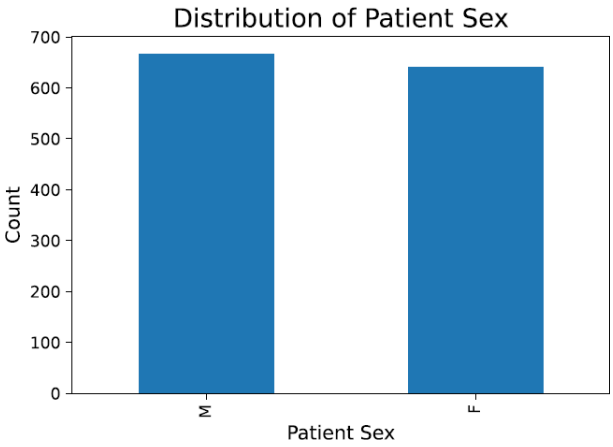


*View/position characteristics*

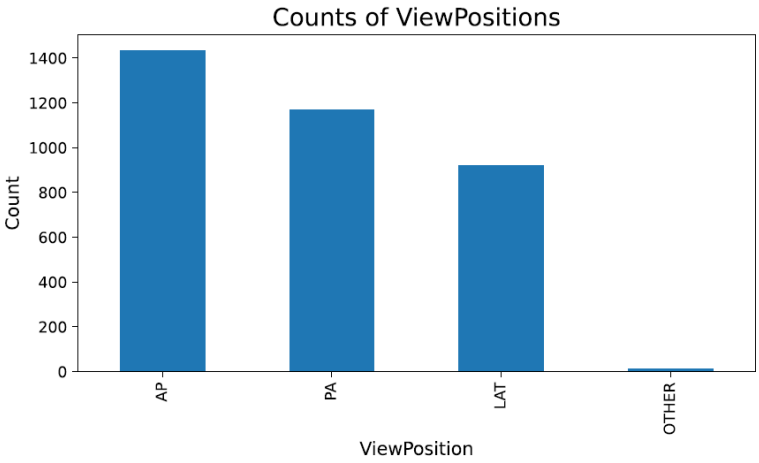


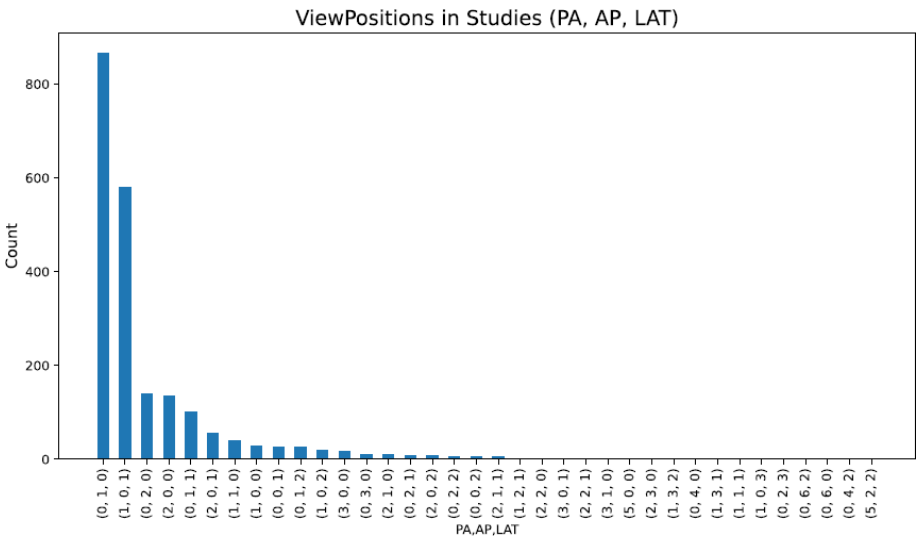

| | |
|---|---|
| Dataset characteristics (CTB) | The Annalise Enterprise product is validated on over 2,500 studies (lossless transfer syntax) acquired from a single Australian source (I-MED Radiology Network Limited).<br><br>The test dataset comprised 2,848 studies originating from 2,419 unique patients from a single Australian source (I-MED Radiology Network Limited).<br><br>Mean patient age was 63.9 years (standard deviation 18.2).<br><br>Distribution of patient sex was 1,524 male (53.5%), 1,322 female (46.4%) and 2 undisclosed. |

*Patient age*

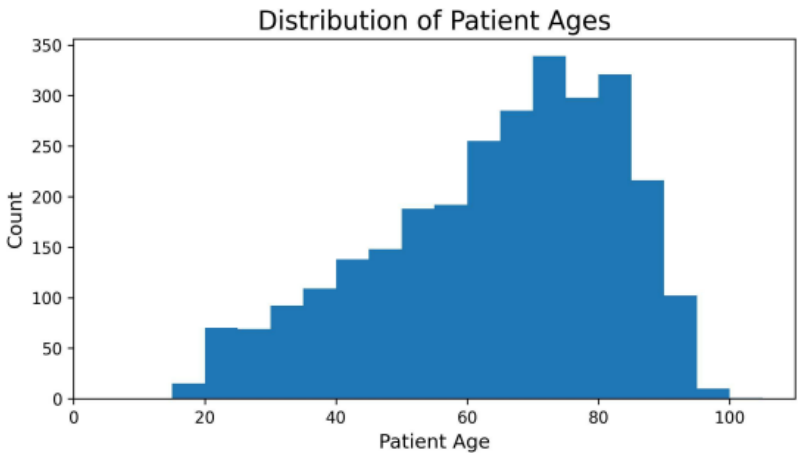


*Patient sex*

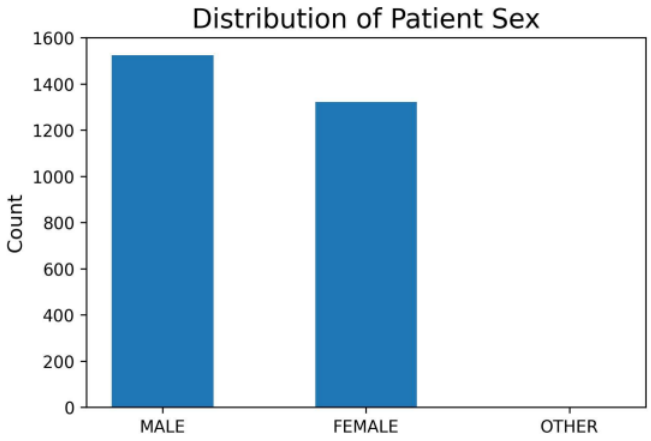

# Acquisition modality of images (CXR)

Overview

The Acquisition Modality is an important marker of image quality.

Computed Radiography (CR) is an older technology which records information on a phosphor cassette prior to digitisation, while Digital Radiography (DX) records and digitises information at the detector, leading to improved spatial resolution.

Decreased spatial resolution may lead to difficulty in distinguishing fine detail on X-rays (such as rib fractures or lung nodules).

Acquisition modality

The following graph displays the distribution of acquisition modalities:

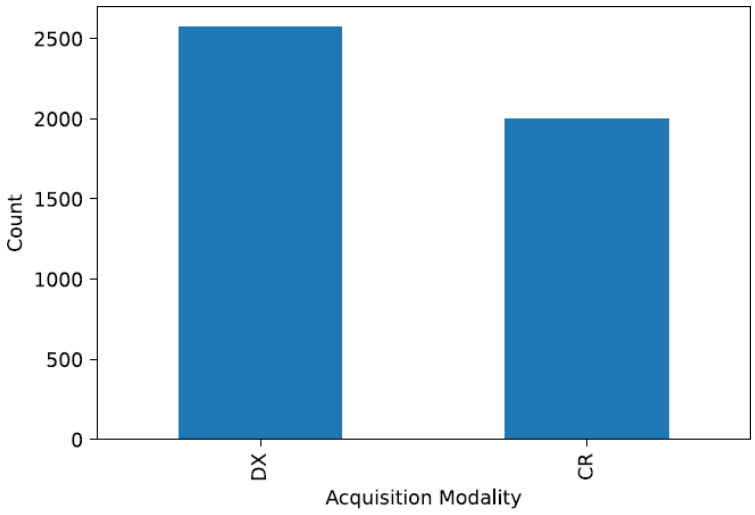

# Imaging device

Overview

This section outlines the distribution characteristics of:

- detector type (CXR)
- imaging device manufacturers (CXR and CTB)
- imaging device models (CXR and CTB)

Detector type (CXR)

When digital radiography is used, the type of detector also changes the image quality.

Scintillator detectors are older technologies which convert X-ray photons to visible photons via scintillation crystals, while direct detectors detect X-ray photons without an intermediate step.

Direct detectors tend to have improved modulation transfer function and spatial resolution. Decreased spatial resolution may lead to difficulty in distinguishing fine detail on X-rays (such as rib fractures or lung nodules).

The following graph displays the distribution of detector types of radiographs:

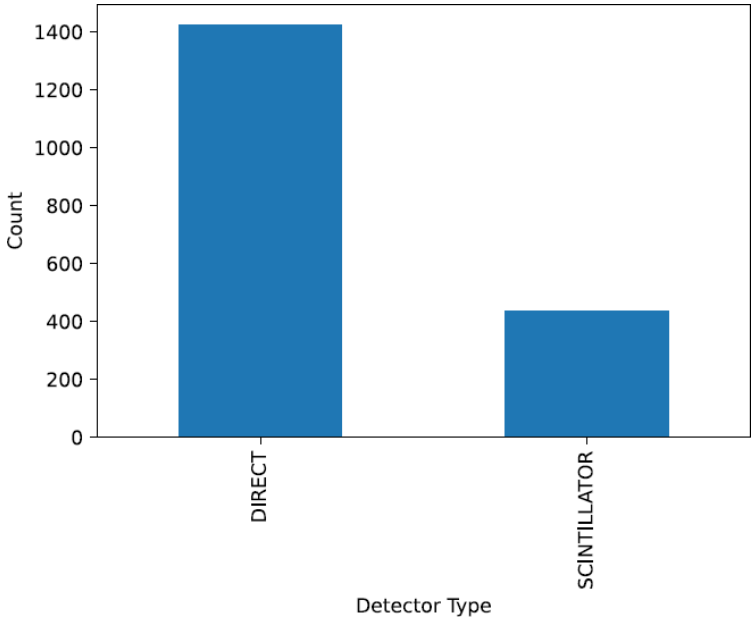

Imaging device models and manufacturers (CXR)

The following graphs display the distribution of CXR imaging device models and manufacturers:

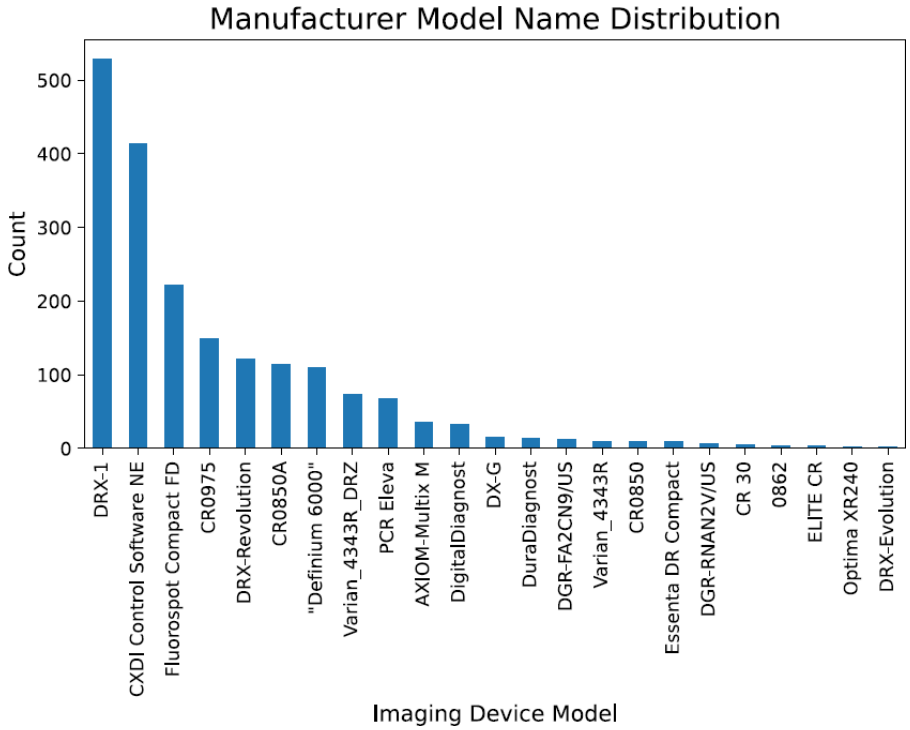


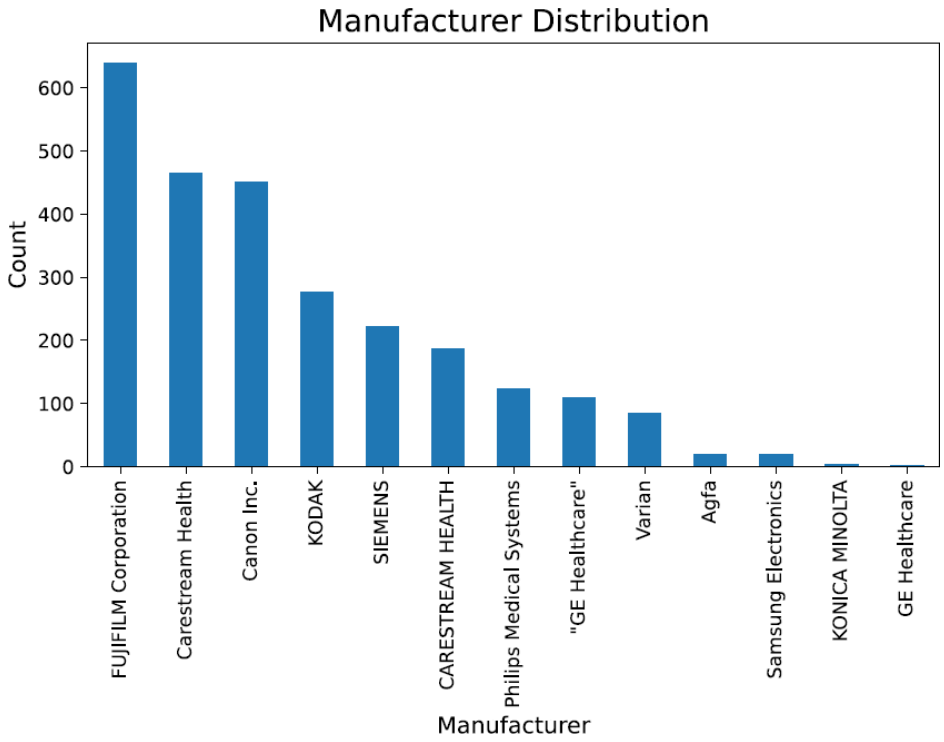

Imaging device models and manufacturers (CTB)

The following graphs display the distribution of CTB imaging device models and manufacturers:

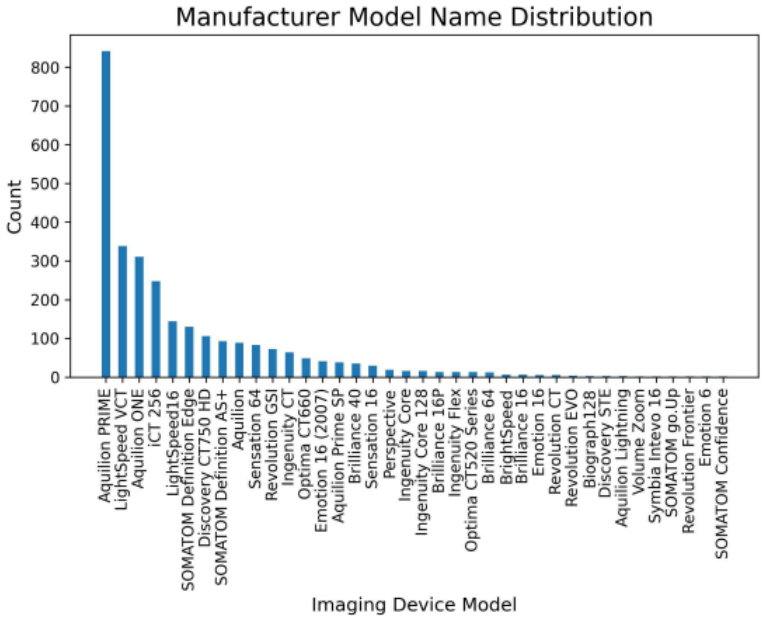


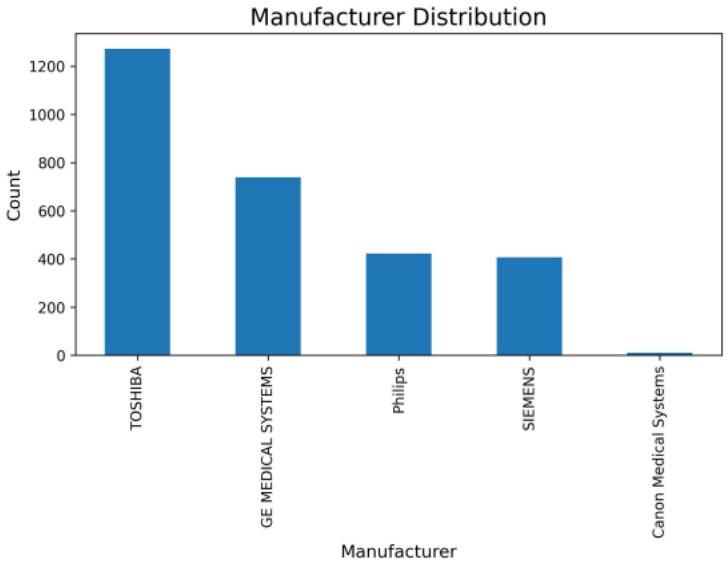

# Distribution of peak kV (CXR)

Overview

The peak kilovolt (KVP) is selected by the radiographer at the time of imaging and can affect image quality.

With automatic exposure control in most systems, higher KVP leads to more X-rays passing through the body and reaching the detector, reducing dose but also reducing contrast resolution.

Lower KVP improves contrast resolution but increases dose to the patient. Too high KVP may lead to difficulty in distinguishing low contrast structures like lung opacities.

Results

The following graphs display the peak voltage in kV for frontal and lateral views:

*Frontal views*

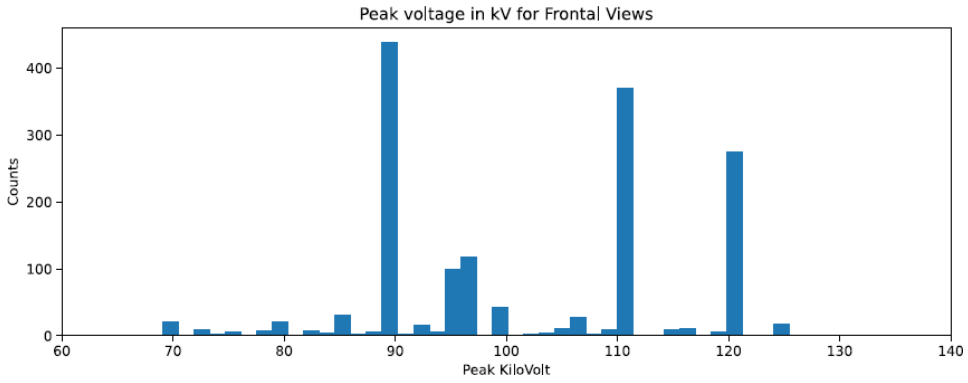


*Lateral views*

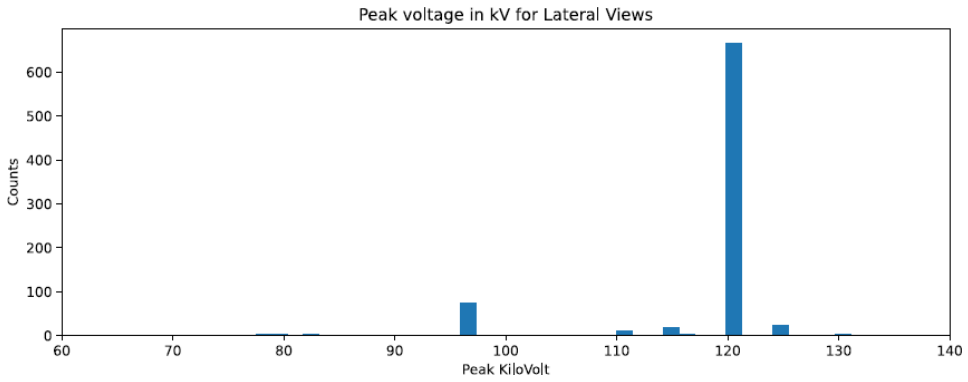

# Distribution of exposure in uAs (CXR)

Overview

The exposure in micro-ampere-seconds (uAs) is the total output of the X-ray tube and is usually automatically controlled by using automatic exposure control. This aims to maintain image quality while reducing exposure as low as reasonably achievable.

Therefore, lateral views will require more exposure where there is more tissue for the X-ray photons to pass through.

Changing the exposure manually will change the Exposure Index (EI) and Deviation Index (DI).

Results

The following graphs display the exposure in uAs for frontal and lateral views:

*Frontal views*

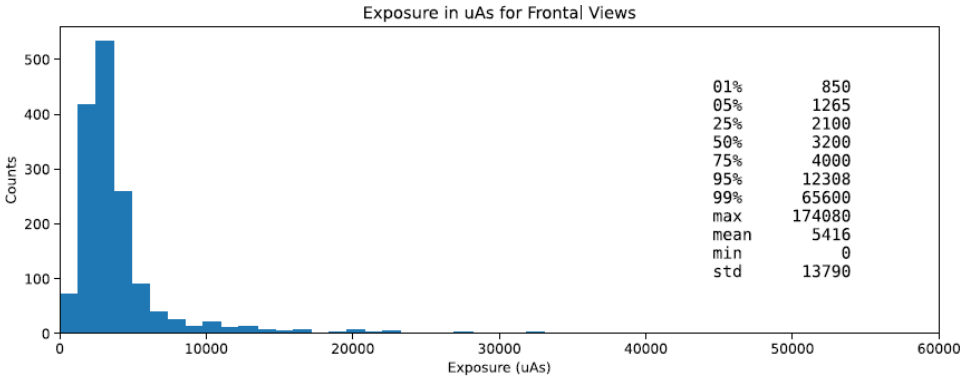


*Lateral views*

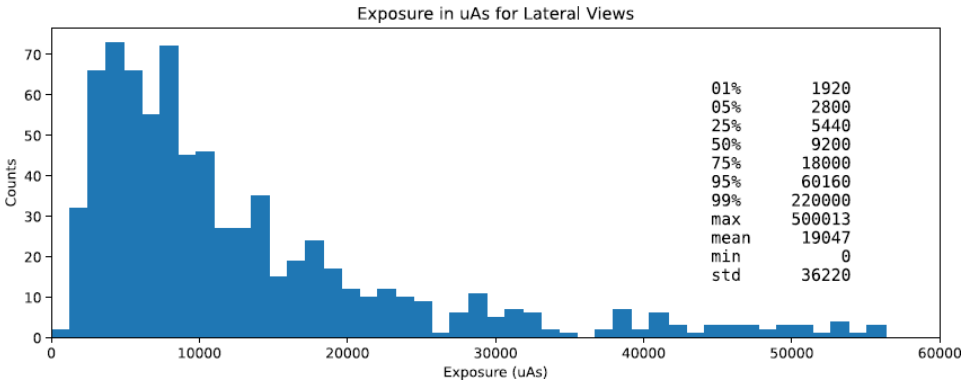

# Radiograph quality indices (CXR)

Overview

The Exposure Index (EI) is a measure of the incident radiation on the detector plate. When automatic exposure control (AEC) is used, it should be roughly similar within the same exam type (for example, frontal chest radiographs) as AEC aims to maintain exposure at a target exposure index.

The Deviation Index (DI) is a logarithmic measure of the difference between the target exposure index and the actual target exposure. High deviation index indicates overexposure while low deviation index indicates underexposure (likely to cause the image to appear more white than necessary).

Different EIs and DIs may lead to difficulty in visualising structures with poor contrast resolution (such as lung opacities).

Results

The following graphs display the exposure index for frontal and lateral views and the deviation index for frontal and lateral views:

*Exposure index for frontal views*

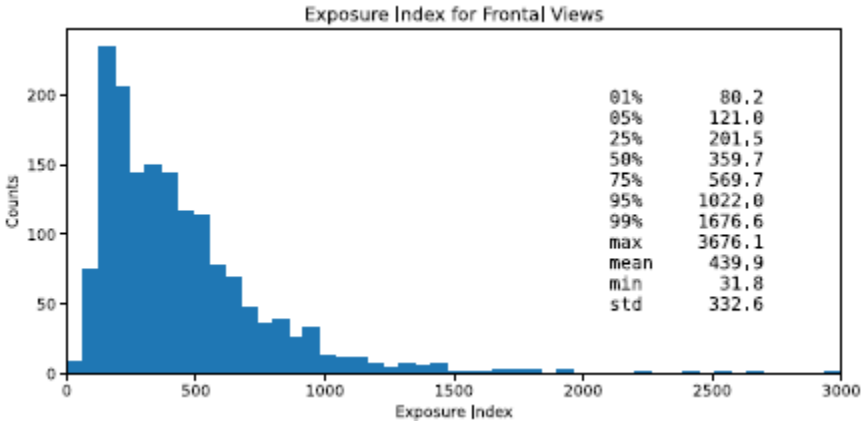


*Exposure index for lateral views*

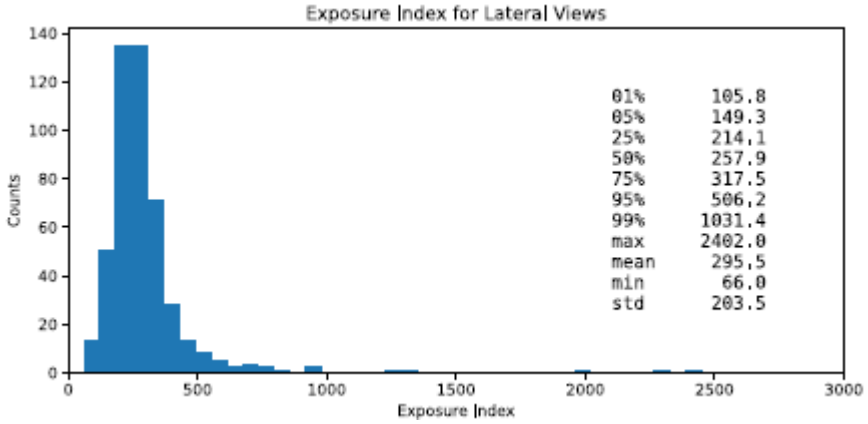

*Deviation index for frontal views*

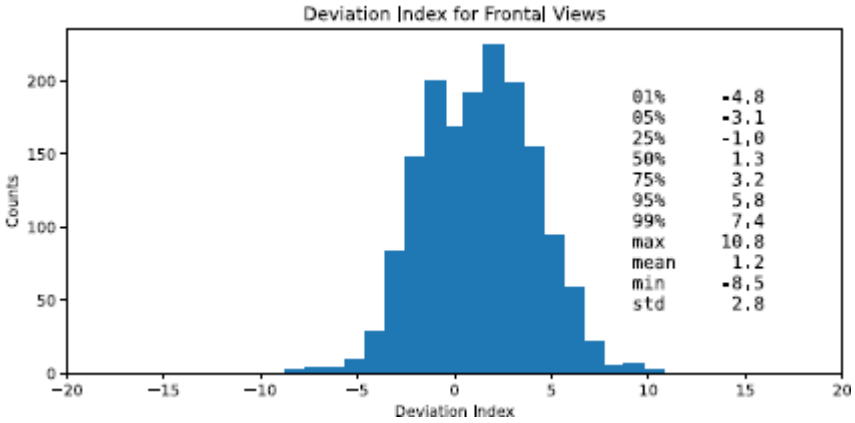


*Deviation index for lateral views*

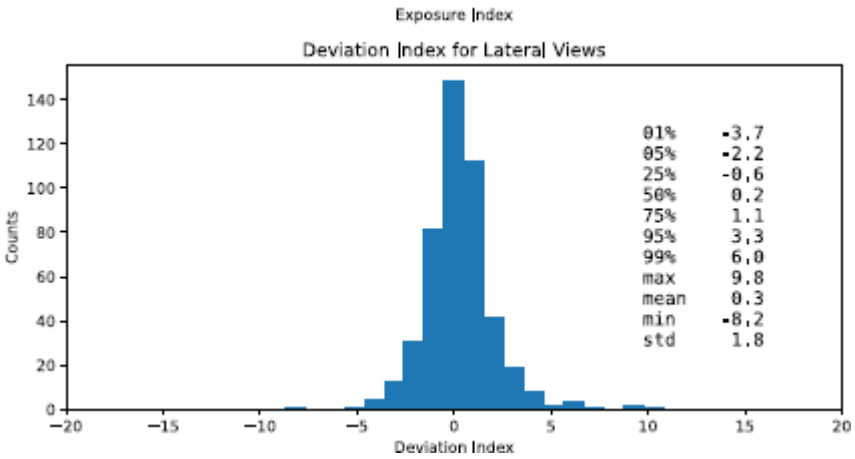

# Pixel spacing values

| | |
|---|---|
| Overview | Pixel spacing is the measure of the physical distance between each recorded pixel on the detector. It is not adjusted for geometric magnification.<br><br>Higher pixel spacing values typically indicate improved spatial resolution unless post-processing has been applied to the image.<br><br>Decreased spatial resolution may lead to difficulty in distinguishing fine detail on X-rays (such as rib fractures or lung nodules) and CT scans (such as subtle bleeds and fractures). |
| Pixel spacing values (CXR) | The following graph displays the pixel spacing values for cases in the dataset: |

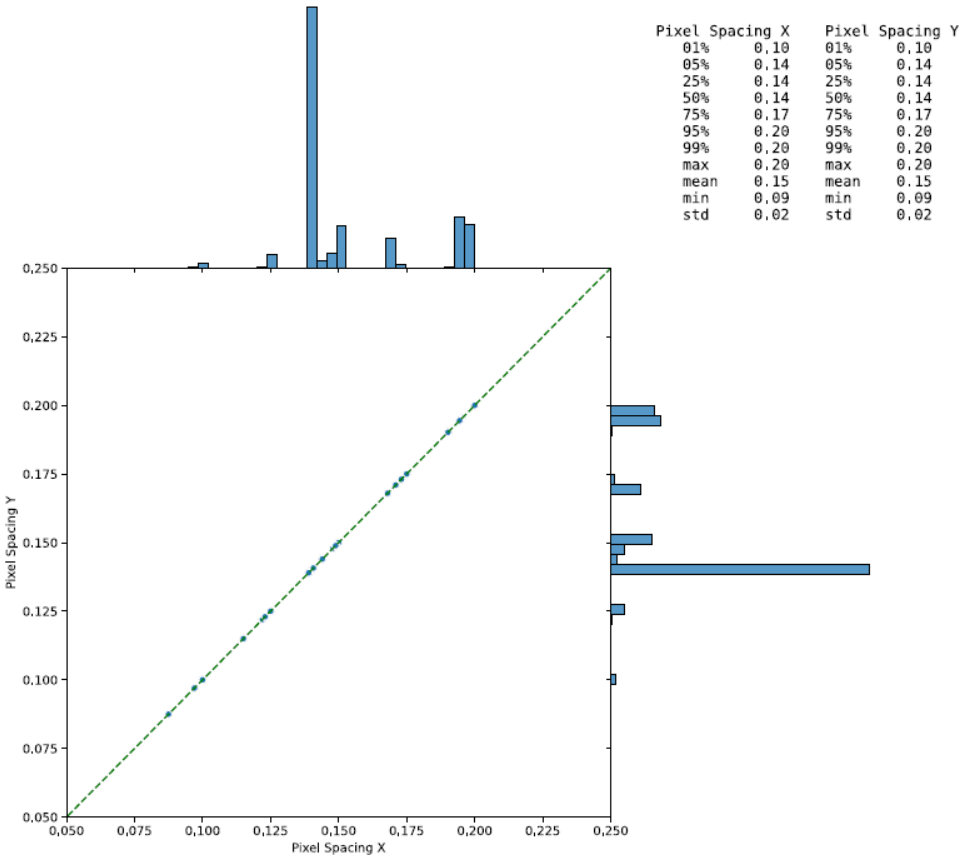

Pixel spacing values (CTB)

Distribution of pixel spacing ranged from 0.65 mm (max) to 0.31 mm (min) with a mean of 0.43 mm across all images (standard deviation 0.03).

The following graph displays the pixel spacing values for the cases in the dataset:

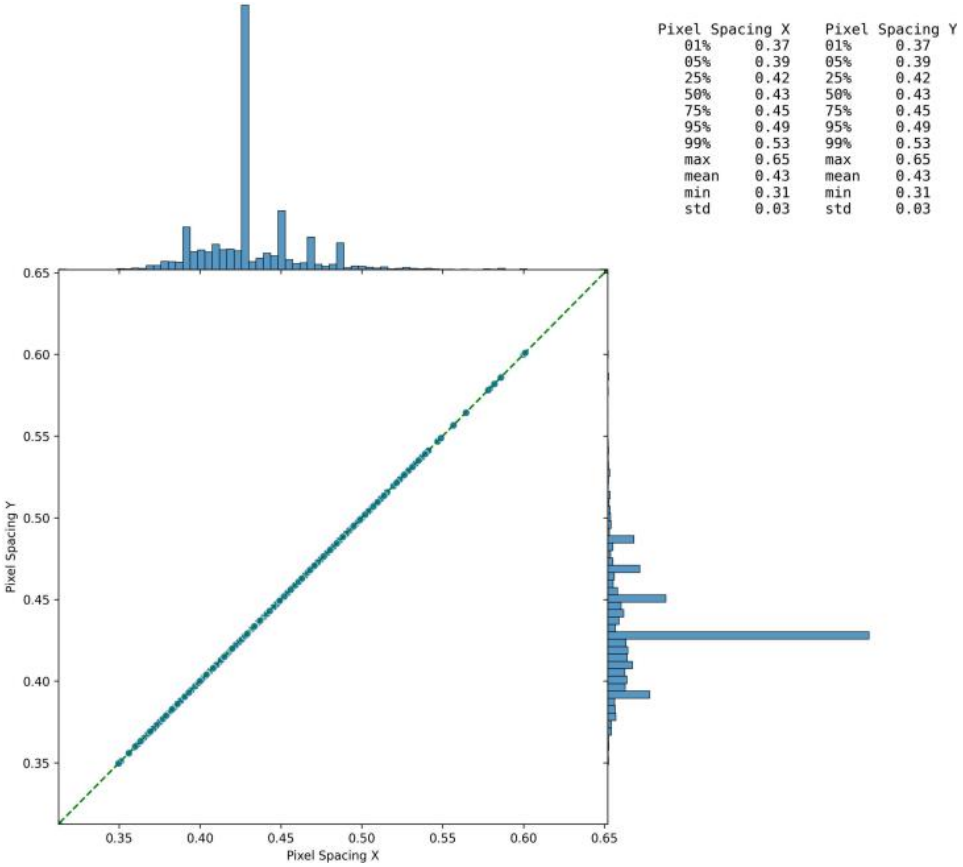

# Support and feedback

## Support and feedback

Refer to the following table for support and feedback details:

| Support type | Details |
|---|---|
| Professional services, technical support and feedback | Email *support@annalise.ai* |
| Product feedback and complaints | Report any product feedback and complaints related to Annalise Enterprise to the Annalise Quality team at email *QA@annalise.ai*.<br>Any serious incidents related to Annalise Enterprise should be reported to annalise.ai and the competent authority or regulatory authority in which the user and/or patient is established. |
| Product user, performance and administration guides | Check our website:<br>*annalise.ai/guides* |

## Symbol glossary

Definitions of symbols that may appear on the Annalise product or in the related documentation are listed below.

| Symbol | Information |
|---|---|
|  | CE labelling in accordance with EC directive |
|  | UK Conformity Assessed marking |
|  | Manufacturer |
|  | European Authorised Representative |
|  | Indicates a warning or caution |
|  | Read the instructions for use |
|  | Medical Device |
| 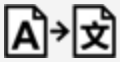 | Translation |

ANNALISE-AI PTY LTD,
Level 21, 60 Margaret Street,
Sydney, NSW 2000
AUSTRALIA

support@annalise.ai
www.annalise.ai

OPT-PRM-029 Ver.2